Frequency Domain Analysis of Laser and Acoustic Pressure Parameters in Photoacoustic Wave Equation for Acoustic Pressure Sensor Designs

Timucin Emre Tabaru[1], Sekip Esat Hayber[2], and Omer Galip Saracoglu[1,3]*

[1]*Clinical Engineering Research and Application Center, Erciyes University, Kayseri 38039, Turkey*
[2]*Department of Electronic and Automation, Ahi Evran University, Kirsehir 40300, Turkey*
[3]*Department of Electrical and Electronic Engineering, Erciyes University, Kayseri 38039, Turkey*

A pressure wave created by the photoacoustic effect is affected by the medium and by laser parameters. The effect of these parameters on the generated pressure wave can be seen by solving the photoacoustic wave equation. These solutions which are examined in the time domain and the frequency domain should be considered by researchers in acoustic sensor design. In particular, frequency domain analysis contains significant information for designing the sensor. The most important part of this information is the determination of the operating frequency of the sensor. In this work, the laser parameters to excite the medium, and the acoustic signal parameters created by the medium are analyzed. For the first time, we have obtained solutions for situations which have no frequency domain solutions in the literature. The main focal point in this work is that the frequency domain solutions of the acoustic wave equation are performed and the effects of the frequency analysis of the related parameters are shown comparatively from the viewpoint of using them in acoustic sensor designs.

I. INTRODUCTION

Pulsed laser photoacoustic (PA) methods offer significant advantages such as detection sensitivity when they are compared with other optical absorption techniques including near-infrared and mid-infrared transmission and reflectance spectroscopy, polarimetry, frequency-domain reflectance technique, spatially-resolved diffuse reflectance technique, light scattering techniques, filter-based photo-absorption techniques. In the PA method, the physical effect caused by absorption is highly sensitive to medium parameters and to their changes. Therefore, the detection sensitivity of the PA method to detect these changes is much higher than other techniques based on the optical absorption. Pulsed laser PA methods are widely used in applications

such as analysis and material characterization due to the detection sensitivity. When any change in the substance content occurs, the acoustic pressure wave is affected by this change. An acoustic detection system can be designed when the sensing of this change is associated with the parameter causing the change.

The method of PA detection involves two challenging processes, namely the production and detection of an acoustic wave. Short pulse widths (in ns or sub-ns) which are implemented by the Pulse Width Modulation (PWM) method must be applied for the laser control to stimulate the medium. It is also necessary to adjust the repetition frequency of the laser. These operations require complex design processes in the construction of electronic devices. A critical design challenge is that the amplitude and transit

---

Color versions of one or more of the figures in this paper are available online.

time of the acoustic wave that modulates with the medium parameters is very low (sub-mV) and short (sub-μs), respectively. Since the amplitude of the generated signal is quite weak, it is inevitable that the signal will be exposed to the medium noise. The laser parameters such as pulse duration, beam width, wavelength, fluence and the acoustic signal parameters such as amplitude, resonance frequency, and bandwidth must be known so that the design challenges can be overcome in a robust way and as a result the signal can be obtained correctly.

The first studies on the PA detection field were carried out in the 1970s by Lahmann *et al*. [1]. They performed a PA method by using an argon ion laser for detecting nonfluorescent absorbers in aqueous solution with a sensitivity of 12 ppt. Oda *et al*. [2] detected cadmium with 14 ppt precision using the pulsed laser PA method. Additionally, they determined the concentrations of the solutions formed with the different types of the food dyes using the same method in another study [3]. The other interesting applications of the photoacoustic sensing up to 1986 can be found in TAM's work [4]. In the 1990s, a CO_2 laser was used in non-destructive testing of solid materials by Davies *et al*. [5]. MacKenzie and co-workers [6-9] performed many trials to detect glucose noninvasively. In the 2000s, this method was also frequently used for gas analysis applications [10-13]. As a different application, Choi *et al*. [14] developed a Doppler velocity meter using a photoacoustic system which operates with CO_2 laser. With this system, they detected a Doppler frequency shift that can be as little as 50 kHz and also found a proper linear relationship between the speed and the shift. In the following years, McCurdy *et al*. [15] showed the applications of breath analysis in a review study up to 2007. Yin *et al*. [16] detected the amount of CO_2 by PA spectroscopy using a near infrared (NIR) laser diode with a sensitivity of 1.556×10^{-8} $W \cdot cm^{-1}/Hz^{(1/2)}$.

The acoustic pressure wave created by the PA effect is widely used in imaging applications. Although the frequency domain analysis of the PA wave equation is used in recent studies on the imaging applications [17, 18], the time domain analysis of the PA wave equation is still used predominantly in the most imaging studies [19, 20]. So, the frequency domain analysis is out of the scope of most imaging studies. Because of the fact that the applications where the PA effect is used are not limited to imaging, nowadays frequency analysis is becoming important in the acoustic sensor design, which is sensitive to the frequency of the acoustic wave generated in the laser-stimulated medium. The frequency domain analysis is performed by means of the frequency solution of the wave equation. There are different approaches in the literature for solving this wave equation. Sigrist *et al*. [21] investigated the effect of different laser pulse durations and the laser beam widths on the solution of the acoustic wave equation. Lai *et al*. [22] summarized the convolution integral of the temporal and radial distributions of the optical density in

a single-effect temporal distribution. Hoelen *et al*. [23] improved Sigrist's model for Gaussian spatiotemporal source generation by using different geometries of the absorption distributions. Calasso *et al*. [24] used the Dirac delta function as the heat function and determined the nonlinear wave equation for the d'Alembert solution at the far field acoustic pressure. Wang *et al*. [25, 26] solved the general PA wave equation using the Green's function approximation and they utilized the Dirac delta function as the source. Some of these approaches are further developed versions of the earlier ones [21, 22]. In addition to the approximate solutions, Erkol *et al*. [27, 28] analytically obtained Gaussian rectangular and radial form solutions in 2013 without using any approximation.

In this study, first we make a rigorous analysis of the time domain approaches and the solutions in order to be used in the acoustic sensor designs. In particular, the results of these solutions have been obtained and the effects of the laser and the acoustic signal parameters at different values and boundary conditions on the PA wave are analyzed as well. Since the acoustic wave amplitude is incredibly low (in μPa) in the medium stimulated by the laser pulses, the resonance frequencies of both the sensor and the acoustic wave formed in the medium should be close to each other. These sensors are known as a narrowband high sensitivity acoustic sensors [29, 30]. They highly increase the acoustic pressure sensitivity and the frequency selectivity of the sensor. Moreover, if the frequency selectivity of the acoustic sensor is high, the frequency response of the material to be detected among the different frequency responses that occur in complex and dynamic media can be easily determined [31]. There are different studies in the literature investigating the acoustic sensor frequency selectivity. For example, the frequency selectivity is an important part of human auditory applications [32]. Yufei Ma *et al*. [33] demonstrated a hydrogen chloride sensor based on the sensitive quartz-enhanced photoacoustic spectroscopy by using a quartz tuning fork (QTF) with a resonance frequency of 30.72 kHz. In their study, they improved the immunity of the obtained signal to the acoustic noise of the medium by increasing the frequency selectivity with a narrow band QTF. The importance of the acoustic frequency selection has been emphasized in these studies. Consequently, the frequency analysis in the acoustic sensor design becomes critical. In addition to the time domain analysis, we obtained secondly frequency domain solutions for the first time in the literature using Fourier transforms for two cases where no frequency domain solutions exist. By focusing on these frequency domain solutions of the acoustic wave equation, we analytically showed the effects on the frequency response of the PA wave for different values of the above-mentioned parameters and we performed the comparative analysis. Through this work we aim to create a new vision using the frequency domain solution of the PA wave equation for future PA sensor designs beyond the analysis.

II. PHOTOACOUSTIC EFFECT
AND ITS THEORY

The main mechanism of the PA effect is to apply low energy level laser pulses to an absorbing medium and to create an acoustic wave propagating through it. The power of these pulses is chosen by the parameters which don't disturb the chemical structure of the material and don't create evaporation. The light energy absorbed by the material is converted to heat energy, and this causes the temperature of the irradiated region to increase. The increasing temperature produces a stretch that causes expansion and compression in the medium. This stretch generates a thermoelastic acoustic pressure wave propagating outwardly. The characteristic of the PA wave is determined by the physical parameters of the medium, such as optical absorption constant, thermal expansion constant, specific heat, and the speed of the sound in the material. The amplitude of the acoustic wave is directly proportional to the absorbed energy density while the shape of the wave depends on the laser parameters and boundary conditions [34]. These relations can be clearly understood from the solution of the PA wave equation.

Depending on the above-mentioned medium parameters, the general PA wave equation is given by Eq. (1) [25],

$$\left(\nabla^2 - \frac{1}{v^2}\frac{\partial^2}{\partial t^2}\right)p(\boldsymbol{r}, t) = \frac{\beta}{\kappa v^2}\frac{\partial^2 T(\boldsymbol{r}, t)}{\partial t^2} \tag{1}$$

where $p(\boldsymbol{r}, t)$ represents the PA wave pressure in position $\boldsymbol{r}$ and time t. β is the thermal volumetric expansion constant, κ is the isothermal compressibility, v is the speed of sound, and $T(\boldsymbol{r}, t)$ shows the temperature change in position $\boldsymbol{r}$ and time t. The right side of the equation expresses the laser source forming the acoustic wave while the left side expresses the acoustic wave propagated in the medium [25]. The heat source also consists of two parts: the first one is the temporal part and the second one is the radial part. The temporal part includes the laser parameters which are also the heat sources while the radial part includes the acoustic wave parameters. For this reason, the wave equation should be solved by adopting different approaches for these parts. So, we focus here on three cases. Although the first case is the most basic solution, the others are chosen because they are considered to be the closest solutions to the exact one. The reason that these cases differ from the each other is the selection of the source functions. In terms of convenience, these are called the first, the second, and the third cases.

Considering these cases and many studies in the literature, the solutions are carried out on an imaginary spherical object heated by the laser as shown in Fig. 1. In addition, these three cases, a boundary condition in Eq. (2) exists between the sensor position $\boldsymbol{r}$, the radius of the heated spherical object R, the speed of the sound v, and the
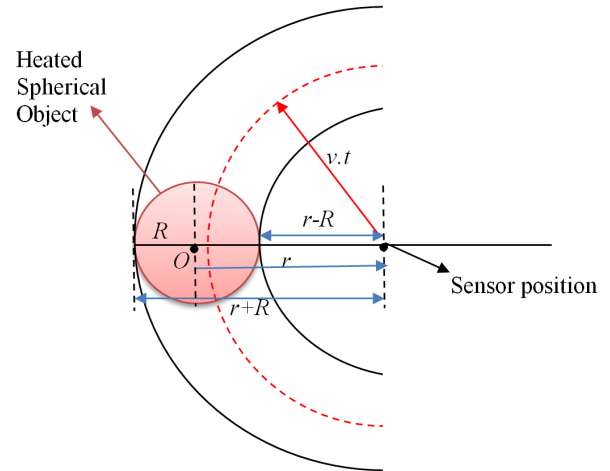

FIG. 1. A spherical object heated by a laser that is thought to exist in the solutions of PA wave equations in the literature.

wave propagation time t. The distance expressed by $v \times t$ will be detected by the sensor as long as it touches the heated spherical object. Otherwise, the acoustic wave will not be detected.

$$\frac{r-R}{v} < t < \frac{r+R}{v} \tag{2}$$

In the first case, the PA wave equation in Eq. (1) is solved by approaching the Green's function [35, 36]. Wang obtained a time domain solution of Eq. (1) using the Dirac delta function of the source term [25]. Then, we have obtained the frequency domain solution of Eq. (1) for $R = 0.5$ mm, $r = 2R$, $v = 1480$ m/s, and $p_0 = 1$ Pa using the inverse Fourier transform of the Wang's time domain solution. The parameters used in this and the following solutions are described in Table 1. The solution is given in Eq. (3).

$$p(r, w) = -\frac{1}{4w^2}\left[\begin{array}{l} -i\exp\left(\dfrac{iw}{7.4\times10^6}\right)w \\[2mm] +i\exp\left(\dfrac{iw}{7.4\times10^6}\right)w + iw \\[2mm] +2.96\times10^6\exp\left(\dfrac{iw}{0.592\times10^6}\right) \\[2mm] -2.96\times10^6\exp\left(\dfrac{iw}{7.4\times10^6}\right) \\[2mm] -2.96\times10^6\exp\left(\dfrac{iw}{1.48\times10^6}\right) \\[2mm] +2.96\times10^6 \end{array}\right]\exp\left(-\dfrac{3iw}{2.96\times10^6}\right) \tag{3}$$

In the second case, Erkol et al. obtained a time domain solution of Eq. (1) from the frequency domain solution by using the inverse Fourier transform. In this solution, the

TABLE 1. Laser, medium, and sensor parameters

Parameters	Description	Unit	Belonging to
R	Radius of heated spherical object	m	Laser
τ	Beam width of the laser	m	Laser
τ_p	Pulse duration	s	Laser
p_0	Initial pressure	Pa	Laser/Medium
v	Speed of sound	m/s	Medium
r	Sensor position	m	Sensor
t	Time	s	-
w	Frequency	Hz	-

temporal part of the source term was regarded as a Gaussian function [27, 28]. Additionally, the temporal and the radial parts of the source term were regarded as the Gaussian function and Heaviside function, respectively. The frequency domain solution of the second case for $r > R$, is presented by Erkol *et al.* and it is given in Eq. (4) [27, 28].

$$p(r, w) = i p_0 \frac{v}{r} \frac{\exp\left(-\frac{\tau_p^2 w^2}{2} + i\frac{w}{v}r\right)}{w^2}\left[\frac{w}{v}R\cos\left(\frac{w}{v}R\right) - \sin\left(\frac{w}{v}R\right)\right]$$

(4)

In the third case, which is the Erkol's solution, both the temporal and the spatial parts of the source function in the time domain solution of the PA wave are chosen as the Gaussian functions. For this reason, a more realistic solution has been achieved than that of the other two cases [27, 28]. The third solution that is called the third case in our study is the main subject of our work and we used Eq. (5) to perform the time domain solution [27, 28].

$$p(r, w) = \frac{p_0}{2\pi}\frac{1}{vr}exp\left(-\frac{\tau_p^2 w^2}{2}\right)$$
$$\times \left\{\int_0^R r' \exp\left(-\frac{r'^2}{2\tau^2}\right)\left[\exp\left[i\frac{w}{v}(r-r')\right] - \exp\left[i\frac{w}{v}(r+r')\right]\right]dr'\right\}$$

(5)

The exponential expressions in the integral of the right-hand side of Eq. (5) are expanded with the Taylor series from 2nd order. In order to compensate for the convergence errors, the expansion is combined with the error function erfi(x). By integrating this result within the specified bounds, we analytically solved Eq. (5) to obtain the frequency domain solution. To our knowledge, this solution is not available in the literature and is given for the first time in this work by Eq. (6). Equation (5) is still useful for computer-based calculations. However, from an engineering point of view, Eq. (6) that is proposed approach in our work is simple enough to embed into a basic microcontroller program code. This makes the sensor design a compact system and independent from the computer.

$$p(r, w) = \frac{p_0}{4\pi}\frac{\tau^2}{v^2 r}\left\{2\exp\left(\frac{R^2 + \frac{\tau^4 w^2}{v^2}}{2\tau^2}\right)\left(-1 + \exp\left(\frac{2iRw}{v}\right)\right)v\right.$$
$$+ \exp\left(\frac{R^2}{\tau^2} + \frac{iRw}{v}\right)\sqrt{2\pi}\,\tau w erfi\left(\frac{-iRv + \tau^2 w}{\sqrt{2}\,\tau v}\right)$$
$$\left.- \exp\left(\frac{R^2}{\tau^2} + \frac{iRw}{v}\right)\sqrt{2\pi}\,\tau w erfi\left(\frac{iRv + \tau^2 w}{\sqrt{2}\,\tau v}\right)\right\}$$
$$\times \exp\left(-\frac{\tau_p^2 w^2}{2} - \frac{R^2}{\tau^2} - \frac{iRw}{v} + \frac{w(2irv - \tau^2 w)}{2v^2}\right)$$

(6)

We have obtained the solutions for the first and the third cases in the frequency domain. The solution for the second case is available in the literature [28, 37].

III. RESULTS AND DISCUSSION

In this section, the effects of the laser, the medium, and the sensor parameters that are given in Table 1, on the acoustic pressure wave created by a pulsed laser are examined in two ways to be useful for a practical acoustic sensor design. These are the time domain and the frequency domain studies given in Sections 3.1 and 3.2, respectively.

3.1. Time Domain Analysis

Figures 2 and 3 show the behavior of the acoustic pressure wave according to the time and the sensor position for the first and the second cases, respectively. In all figures, the selected parameter values are $R = 0.5$ mm and $v = 1480$ m/s [25]. As can be seen from Figs. 2 and 3, although the generated the PA wave amplitude is the highest in the time interval between 0.4 μs and 1 μs, it is very difficult to detect the amplitudes between the intervals. The pressure changes in the negative regions in the graphs represent the waves reflected from the center of the spherical object while the positive regions represent the waves diverged. As shown in Figs. 2(b) and 3(b), the position of the sensor should be located within a few millimeters from the
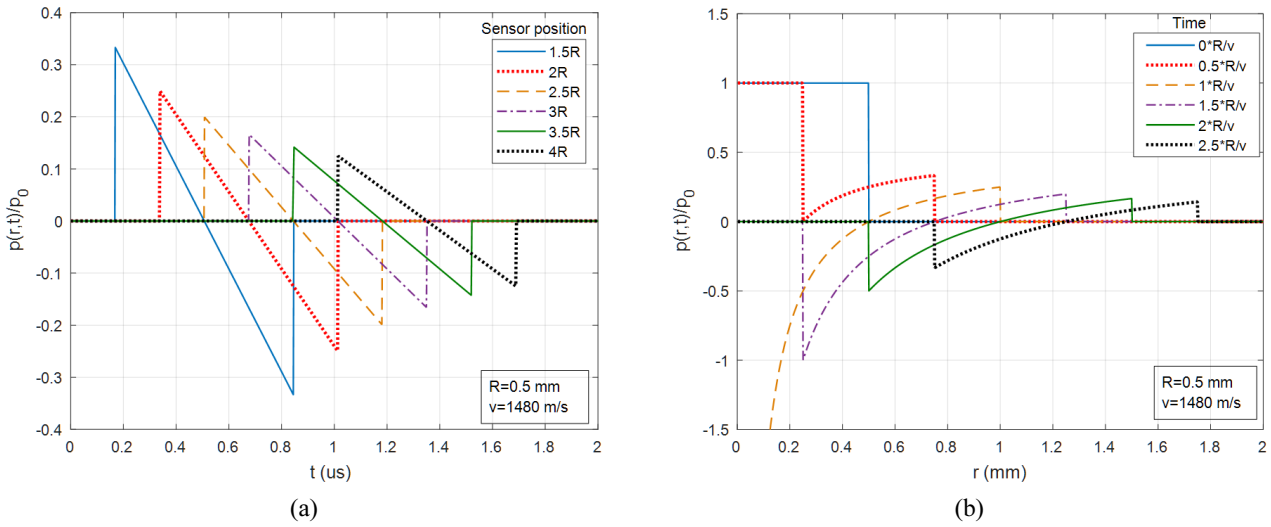
FIG. 2. Normalized pressure of the acoustic wave obtained by the first case for (a) different sensor positions with time (b) different normalized times with sensor position.
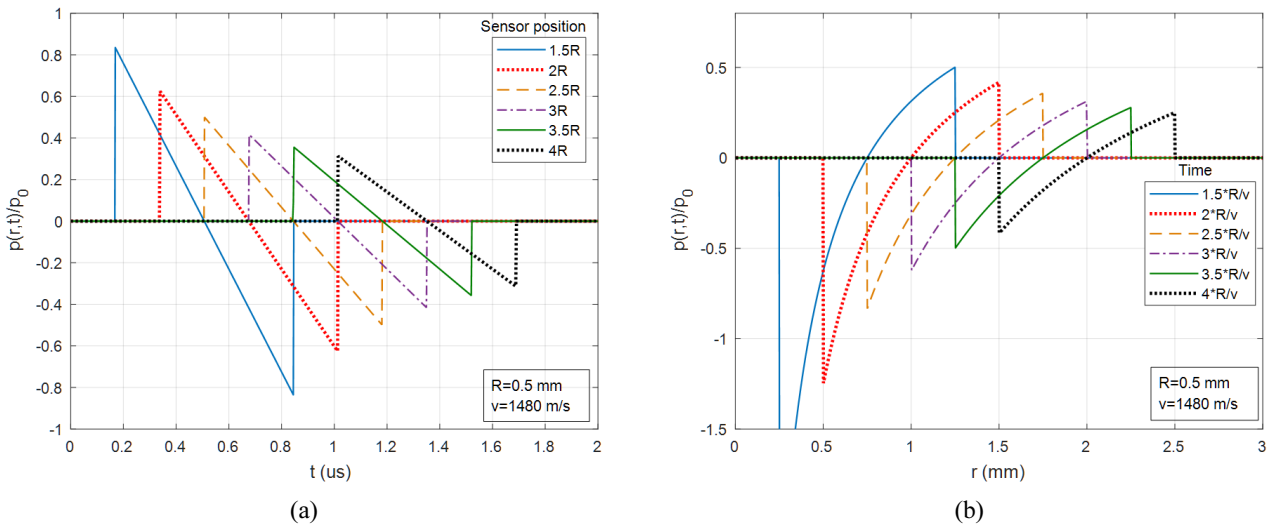

FIG. 3. Normalized pressure of the acoustic wave obtained by the second case for (a) different sensor positions with time (b) different normalized times with sensor position.

heated spherical object for the detection of the PA wave. If it is chosen at the longer distances, the detected signal amplitude will significantly reduce. In addition, after a certain distance, the wave will disappear by damping and won't have been able to detect. In the second case, a pressure wave with the higher amplitude is generated due to the selected source function's effect. In this case, the frequency spectrum expands because of the Gaussian selection of the temporal part of the selected source function and so the spectral content becomes richer. This situation causes different absorptions, moreover, an increase occurs in the amplitude of the resulting acoustic wave.

Time-domain analysis of the third case, which is the most realistic one, is performed according to varying time and positions of the sensor. Figure 4 shows the time-

varying effect of different sensor positions, pulse durations and beam widths on the pressure. In this case, the detected amplitude value is generally less than that of the detected amplitude values in the first and the second cases. However, as the laser beam width increases, the measured amplitude increases as shown in Fig. 4(c), and it approaches to the amplitudes of the other cases. In addition, the high pulse durations further reduce the amplitude values as shown in Fig. 4(b). As shown in Fig. 4(a), the sensor located in the boundary of the heated sphere measures the maximum pressure. As the sensor moves away from this point, the value of the pressure approaches a value which is so small that it cannot be measured. Similar results can be concluded below for Fig. 5 which shows the normalized pressure values in the varying position of the sensor at different
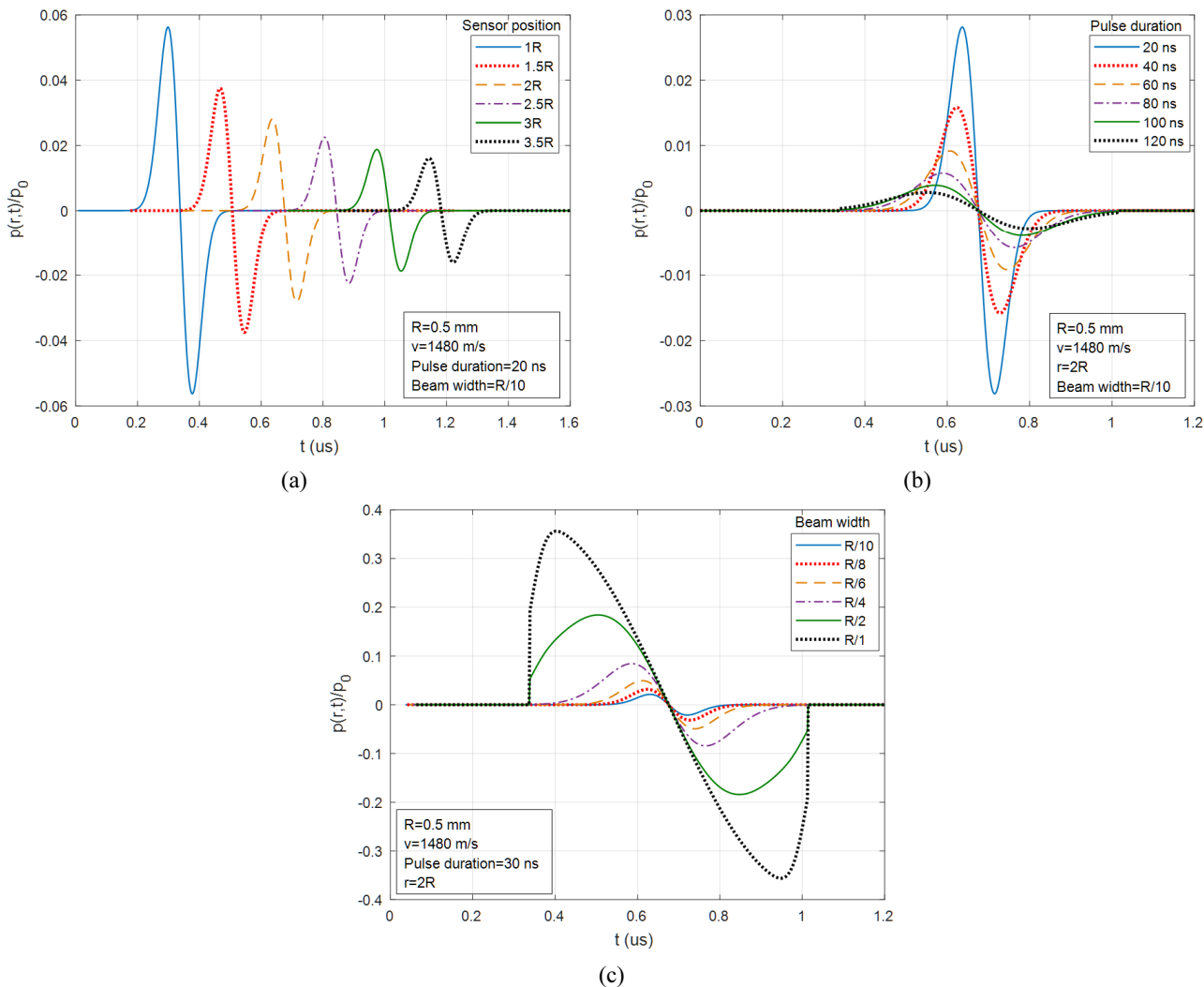
FIG. 4. The normalized pressure values in the varying times for the third case: (a) At different values of r; (b) At different values of τ_p; (c) At different values of τ.
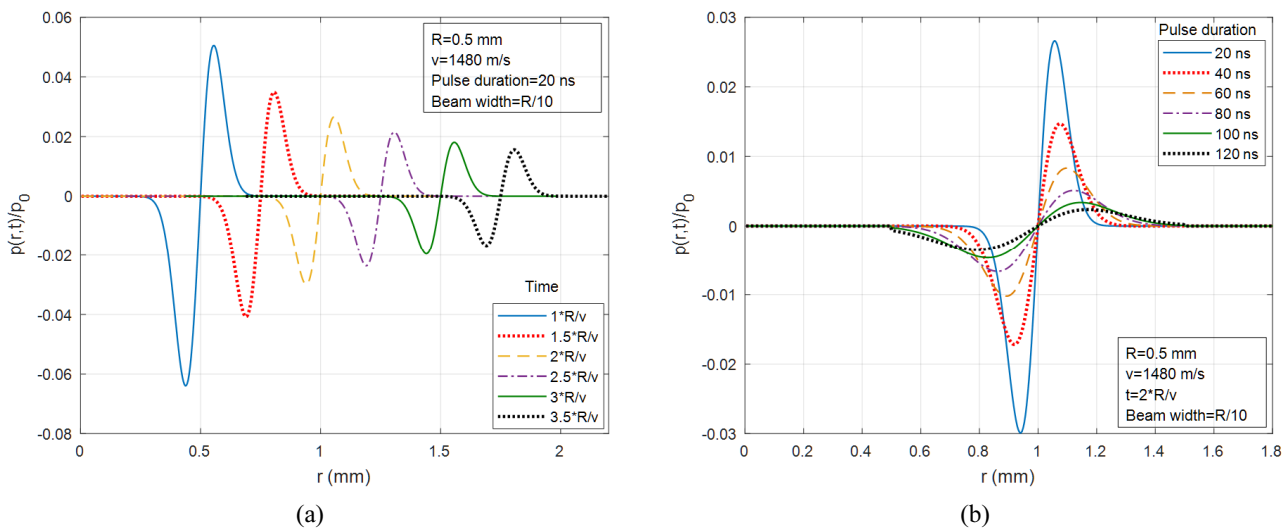

FIG. 5. The normalized pressure values in the varying position of sensor for the third case: (a) At different values of t; (b) At different values of τ_p; (c) At different values of τ.
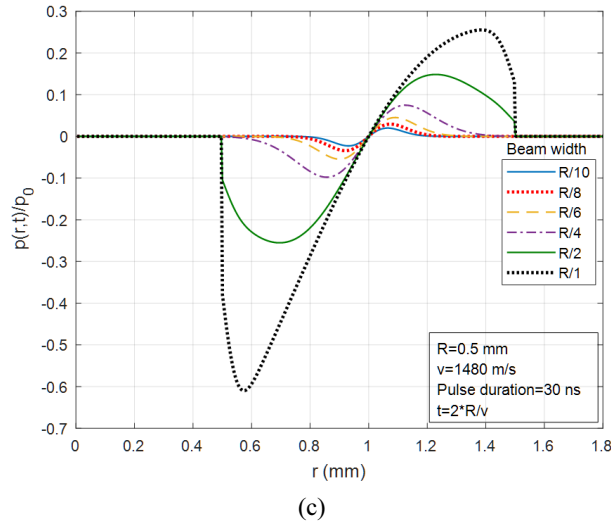
(c)

FIG. 5. The normalized pressure values in the varying position of sensor for the third case: (a) At different values of t; (b) At different values of τ_p; (c) At different values of τ (Continue).

normalized times, pulse durations and beam widths.

Figures 5(a)~5(c) show for the normalized pressure of the third case with the varying position of the sensor at different normalized times, different pulse durations, and different beam widths, respectively. As shown in Fig. 5(a), while the distance and the sensing time increase, the pressure decreases which is a predicted result.

In Fig. 6, a specific sensor position and the measurement time values are selected to be able to see the effect of the laser pulse width and the laser beam width on the formed pressure wave at the same time. It shows that amplitude of the PA wave is reduced with the pulse duration. Because, if the laser energy does not change, the pulse duration and the pulse peak power will be inversely proportional to each other. It means that the shorter the pulse duration, the higher the amplitude of the PA signal. Also, Fig. 6 shows
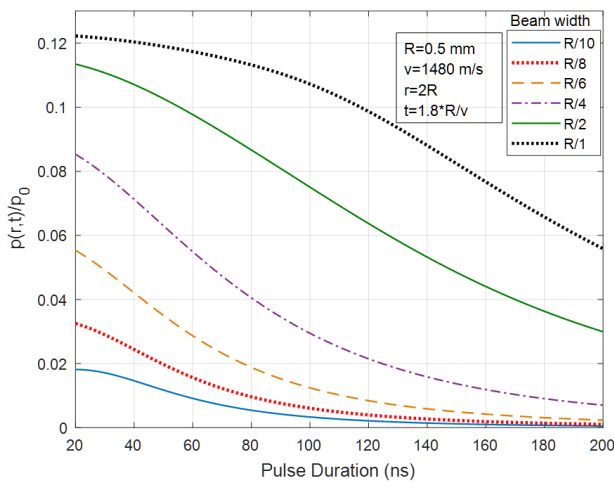
that the change in the PA signal smoothly falls while R/t is rising. This occurs because the radial part is sharpened and behaves like a Dirac delta function. In Figs. 4(c) and 5(c), the incomplete formation of some waves is due to the fact that the selected parameters are outside the boundary condition of Eq. (2) and the sensor cannot detect them.

3.2. Frequency Domain Analysis

Because the applications in which the PA effect is used are not limited to imaging, in the design of an acoustic sensor which is sensitive to the frequency of the acoustic wave generated in laser-stimulated medium, the frequency analysis becomes very critical. The substance or the analyte can be detected with the sensor tuned to the frequency of the desired acoustic wave. The physical nature of the acoustic wave generated by the laser-stimulated medium must be known with all aspects for the acoustic sensor designs. In this section, the frequency domain analyses made in this work are compared. In this comparison the effect of parameters such as the sensor position, the speed of the sound, the acoustic wave measurement time and the laser parameters are investigated and become clearer by the frequency analysis. In this way, it is possible to use these outputs obtained by the solutions of the first and third cases in acoustic sensor designs.

The radius of the heated spherical object, the speed of the sound, the sensor position, and the initial pressure which are shown in Table 1 are common parameters in the three cases and the graphs between Figs. 7 and 10 are drawn with the equal selected values of these parameters. The laser pulse duration is available in the second and the third cases while the laser beam width value is used only in the third case. One can easily observe the effects on the PA pressure by selecting different values of these parameters. In Fig. 7(a), the frequency response of the first

FIG. 6. The effect of the pulse duration on the acoustic wave pressure for the third case at different beam widths.
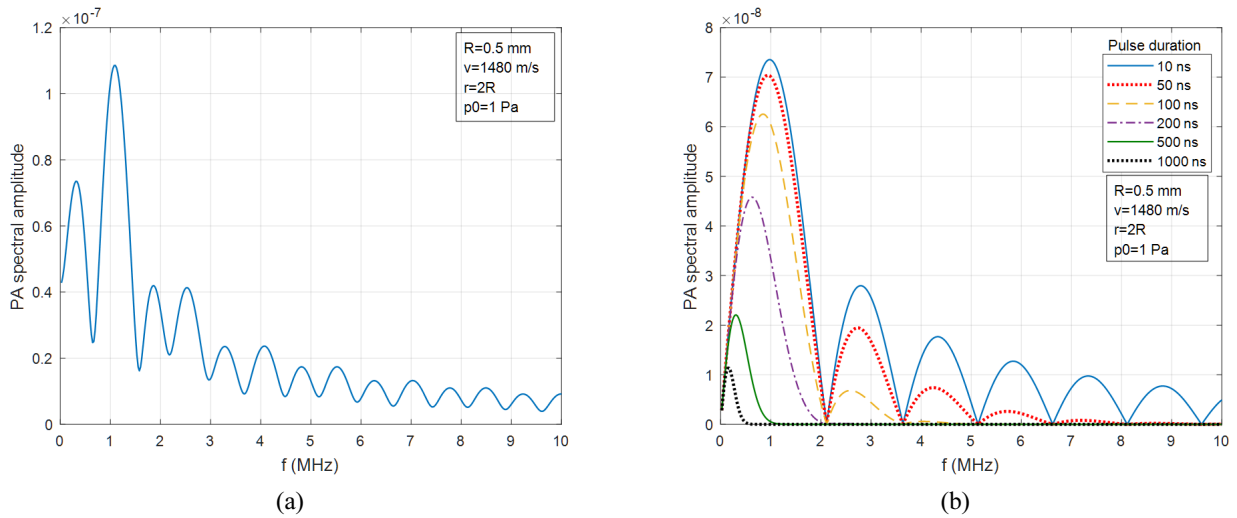
FIG. 7. The frequency response of: (a) the first approach; (b) at different pulse durations for the second approach.
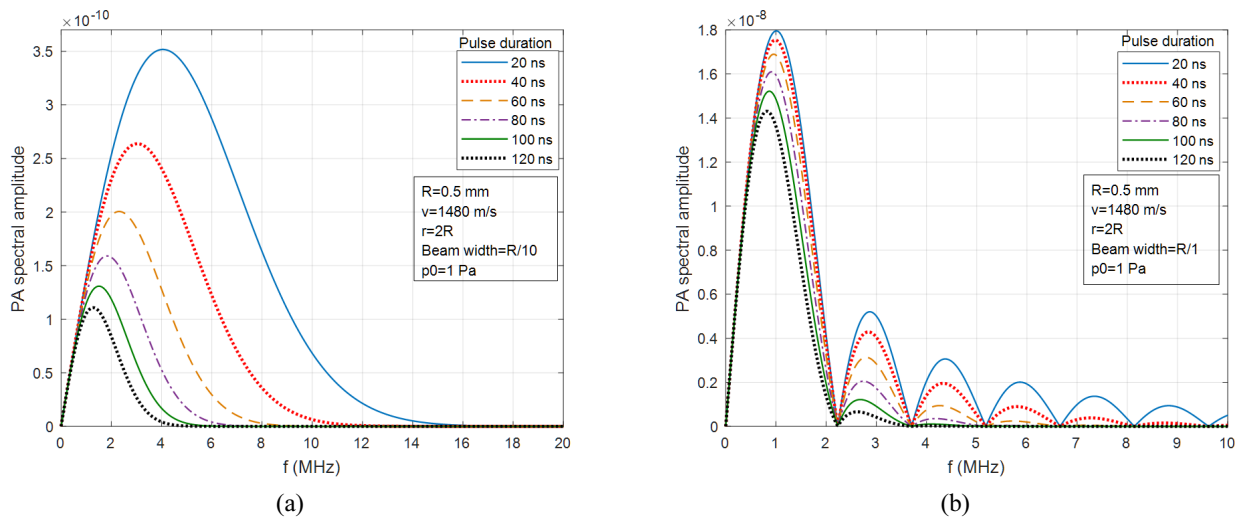

FIG. 8. The effects of the pulse duration on the spectral amplitude of the PA wave: (a) at beam width = $R/10$; (b) at beam width = $R/1$.
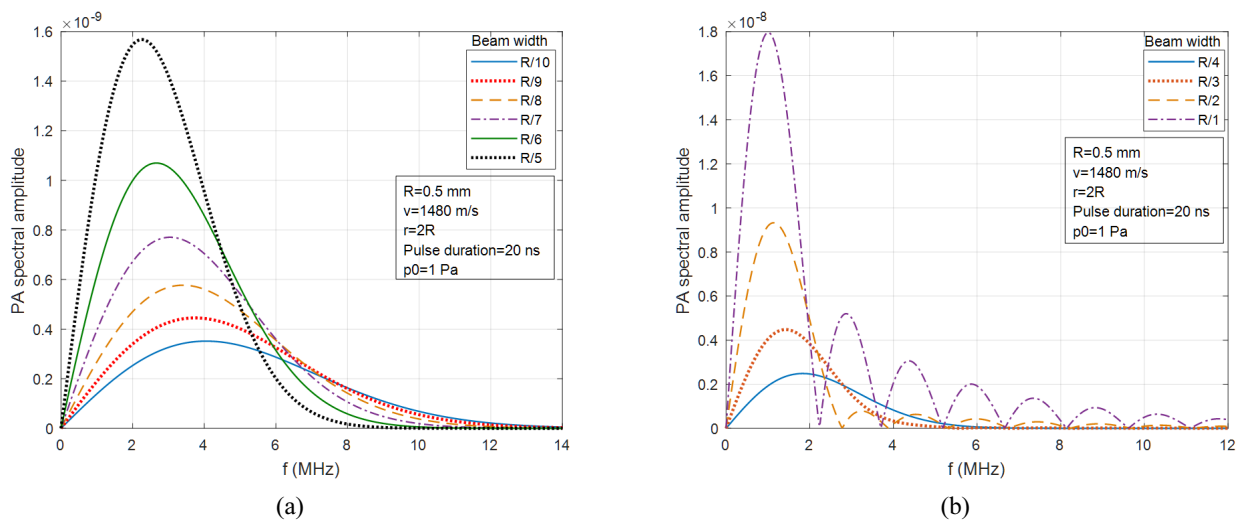

FIG. 9. The effects of the beam widths on the acoustic pressure of the pulse duration = 20 ns for (a) the lower and (b) the higher beam widths.
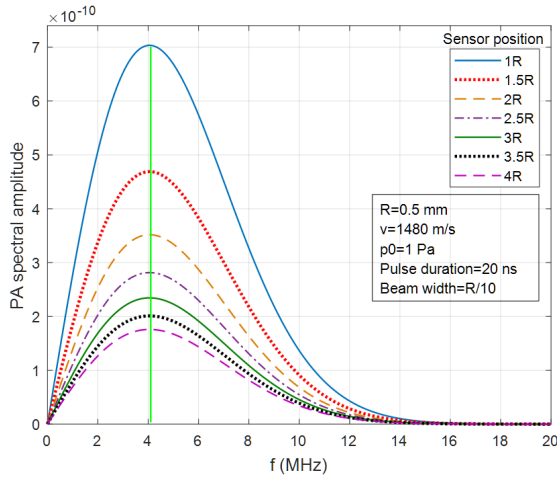
FIG. 10. The frequency response of the third solution at different sensor positions.

FIG. 11. Our proposed approach versus experimental result of K. M. Quan *et al*. [38].

case is examined and in this case the amplitude of the pressure wave is obtained as the highest. The maximum amplitude is numerically detected about 1.1 MHz. In Fig. 7(b), the effect of the pulse duration is shown. Additionally, the amplitude in the second case is lower than the value in the first case. The reducing amplitude with the increasing pulse duration values is a consequence of the losses due to the spreading of the energy absorptions in the medium. Also, as Fig. 7(b) shows, the harmonics occur at the low pulse durations. Another effect of the pulse duration is that the resonance frequency of the acoustic wave decreases as the pulse duration increases. As a numerical example, the frequency value corresponding to the pulse duration 10 ns is about 1 MHz while the frequency value corresponding to 1 μs is about 0.17 MHz. Knowing these values is critical in deciding whether the bandwidth of the acoustic sensor to be created is a broad or a narrow band.

For a practical sensor design, the effect of the laser beam width, can be inserted into account in the third case. At different values of this parameter, the effect of laser pulse duration varies. More clearly, the pulse duration effects of different lasers having a lower and a higher beam width will be different. These are shown in Figs. 8(a) and 8(b). Figure 8(a) shows the low-pressure values at the low beam width and the absence of the harmonics while Fig. 8(b) shows the high-pressure values at the high beam width and the presence of the harmonics. Consequently, it can be concluded that this is a result of the interaction of the laser with a larger surface. It is also clear that the pulse duration increases as the resonant frequency decreases which is shown in Figs. 8(a) and 8(b). A frequency shifting becomes larger when the pulse duration changes at the low beam width of the laser. The frequency increases with increasing beam, however, pressure decreases with increasing beam width as shown in Fig. 9. In addition, since the spectral amplitudes at the lower and the higher values of the beam width are different, the graph is divided into two
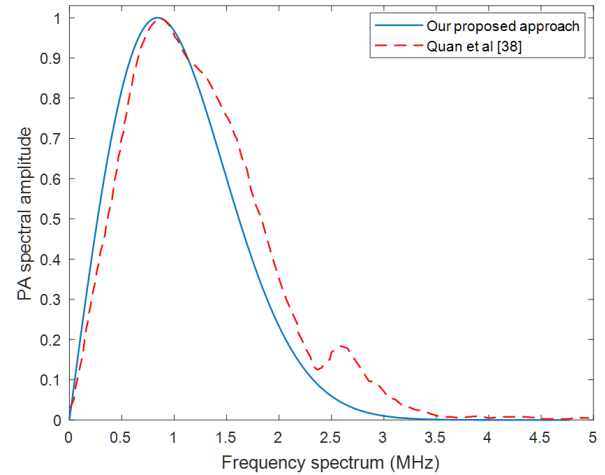
parts as shown in Figs. 9(a) and 9(b). The harmonics occur at high beam widths (Fig. 9(b)) while harmonics do not occur at low beam widths (Fig. 9(a)). This situation shows that as the beam width increases, the spectral content becomes richer.

Figure 10 shows that changing of the sensor position has no effect on the frequency of the generated pressure wave. There occur changes in the amplitudes of the signals with the same resonant frequency where the signals are measured by the sensors at different positions. While pulse duration and beam width shift the resonant frequency, the sensor position does not have any effect on the resonant frequency. This is an important result for an acoustic sensor design. Figure 11 shows the comparison of our proposed approach with the experimental result of Quan *et al*. [38]. The results are obtained by using the parameters specified in Quan's experiment. It can be seen that our results are in good agreement with the experimental results. This suggests that our approach has a high degree of reliability.

IV. CONCLUSION

The solutions obtained by performing different approaches to the photoacoustic wave equation to be useful for a practical sensor design are presented. The frequency domain solutions have been derived from the time domain solutions and the effects of the laser parameters on these solutions have been investigated. The focus is on the most realistic solution and its results, which have been carried out by relating the photoacoustic pressure wave with the medium and the laser parameters, for the sensor designs. It is concluded that the frequency of the generated acoustic wave and the amplitude of pressure both depend on the laser parameters and the medium parameters. Another interesting result is that the frequencies of the PA waves generated are not influenced by the sensor location. So, a

designer can locate the sensor to any point on the medium for the frequency modulated sensing applications. On the other hand, the sensor must be located as nearly as possible to acoustic source for the amplitude modulated sensing applications.

ACKNOWLEDGMENT

REFERENCES

1. W. Lahmann, H. J. Ludewig, and H. Welling, "Opto-acoustic trace analysis in liquids with the frequency-modulated beam of an argon ion laser," Anal. Chem. **49**, 549-551 (1977), doi: 10.1021/ac50012a012.

2. S. Oda, T. Sawada, and H. Kamada, "Determination of ultratrace cadmium by laser-induced photoacoustic absorption spectrometry," Anal. Chem. **50**, 865-867 (1978), doi: 10.1021/acs.analchem.6b03286.

3. S. Oda, T. Sawada, M. Nomura, and H. Kamada, "Simultaneous determination of mixtures in liquid by laser-induced photoacoustic spectroscopy," Anal. Chem. **51**, 686-688 (1979), doi: 10.1021/ac50042a025.

4. A. C. Tam, "Applications of photoacoustic sensing techniques," Rev. Mod. Phys. **58**, 381 (1986), doi: 10.1103/RevModPhys.58.381.

5. S. J. Davies, C. Edwards, G. S. Taylor, and S. B. Palmer, "Laser-generated ultrasound: its properties, mechanisms and multifarious applications," J. Phys. D: Appl. Phys. **26**, 329 (1993), doi: 10.1088/0022-3727/26/3/001.

6. H. A. MacKenzie, G. B. Christison, P. Hodgson, and D. Blanc, "A laser photoacoustic sensor for analyte detection in aqueous systems," Sens. Actuators, B **11**, 213-220 (1993), doi: 10.1016/0925-4005(93)85257-B.

7. H. A. MacKenzie, H. S. Ashton, Y. C. Shen, J. Lindberg, P. Rae, K. M. Quan, S. Spiers, "Blood glucose measurements by photoacoustics," in *Proc. Biomedical Optical Spectroscopy and Diagnostics* (United States, Mar. 1998), paper BTuC1, doi: 10.1364/BOSD.1998.BTuC1.

8. G. B. Christison and H. A. MacKenzie, "Laser photoacoustic determination of physiological glucose concentrations in human whole blood," Med. Biol. Eng. Comput. **31**, 284-290 (1993), doi: 10.1007/BF02458048.

9. H. A. MacKenzie, H. S. Ashton, S. Spiers, Y. Shen, S. S. Freeborn, J. Hannigan, and P. Rae, "Advances in photoacoustic noninvasive glucose testing," Clin. Chem. **45**, 1587-1595 (1999), ISSN: 1530-8561.

10. F. J. Harren, J. Mandon, and S. M. Cristescu, "Photoacoustic spectroscopy in trace gas monitoring," in *Encyclopedia of Analytical Chemistry* (1999), ISBN: 10.1002/9780470027318.

a0718.pub2.

11. A. Elia, P. M. Lugarà, C. De Franco, and V. Spagnolo, "Photoacoustic techniques for trace gas sensing based on semiconductor laser sources," Sensors, **9**, 9616-9628 (2009), doi: 10.3390/s91209616.

12. A. Elia, C. Di Franco, P. M. Lugarà, and G. Scamarcio, "Photoacoustic spectroscopy with quantum cascade lasers for trace gas detection," Sensors, **6**, 1411-1419 (2006), doi: 10.2478/s11534-009-0042-8.

13. A. Miklós, P. Hess, and Z. Bozóki, "Application of acoustic resonators in photoacoustic trace gas analysis and metrology," Rev. Sci. Instrum. **72**, 1937-1955 (2001), doi: 10.1063/1.1353198.

14. J. W. Choi, M. J. You, S. W. Choi, and S. Y. Woo, "Photoacoustic laser doppler velocimetry using the self-mixing effect of RF-excited CO_2 laser," J. Opt. Soc. Korea **8**, 188-191 (2004), doi: 10.3807/JOSK.2004.8.4.188.

15. M. R. McCurdy, Y. Bakhirkin, G. Wysocki, R. Lewicki, and F. K. Tittel, "Recent advances of laser-spectroscopy-based techniques for applications in breathe analysis," J. Breath Res. **1**, 014001 (2007), doi: 10.1088/1752-7155/1/1/014001.

16. X. Yin, L. Dong, H. Zheng, X. Liu, H. Wu, Y. Yang, and S. Jia, "Impact of humidity on quartz-enhanced photoacoustic spectroscopy based CO detection using a near-IR telecommunication diode laser," Sensors **16**, 162 (2016), doi: 10.3390/s16020162.

17. P. Mohajerani, S. Kellnberger, and V. Ntziachristos, "Frequency domain optoacoustic tomography using amplitude and phase," Photoacoust. **2**, 111-118 (2014), doi: 10.1016/j.pacs.2014.06.002.

18. R. E. Kumon, C. X. Deng, and X. Wang, "Frequency-domain analysis of photoacoustic imaging data from prostate adenocarcinoma tumors in a murine model," Ultrasound in Med. Biol. **37**, 834-839 (2011), doi: 10.1016/j.ultrasmedbio.2011.01.012.

19. D. Wu, L. Huang, M. S. Jiang, and H. Jiang, "Contrast agents for photoacoustic and thermoacoustic imaging: a review," Int. J. Mol. Sci. **15**, 23616-23639 (2014), doi: 10.3390/ijms151223616.

20. S. Y. Nam and S. Y. Emelianov, "Array-based real-time ultrasound and photoacoustic ocular imaging," J. Opt. Soc. Korea **18**, 151-155 (2014), doi: 10.3807/JOSK.2014.18.2.151.

21. M. W. Sigrist and F. K. Kneubühl, "Laser-generated stress waves in liquids," J. Acoust. Soc. Am. **64**, 1652-1663 (1978), doi: 10.1121/1.382132.

22. H. M. Lai and K. Young, "Theory of the pulsed optoacoustic technique," J. Acoust. Soc. Am. **72**, 2000-2007 (1982), doi: 10.1121/1.388631.

23. C. G. A. Hoelen, F. F. M. De Mul, R. Pongers, and A. Dekker, "Three-dimensional photoacoustic imaging of blood vessels in tissue," Opt. Lett. **23**, 648-650 (1998), doi: 10.1364/OL.23.000648

24. I. G. Calasso, W. Craig, and G. J. Diebold, "Photoacoustic point source," Phys. Rev. Lett. **86**, 3550 (2001), doi: 10.1103/PhysRevLett.86.3550.

25. L. V. Wang and H. I. Wu, *Biomedical optics: principles and imaging*, John Wiley & Sons (2012), ISBN: 9780470177006.

26. L. V. Wang, "Tutorial on photoacoustic microscopy and computed tomography," IEEE J. Sel. Topics Quantum Electron. **14**, 171-179 (2008), doi: 10.1109/JSTQE.2007.913398.

27. H. Erkol, E. Aytac-Kipergil, M. U. Arabul, and M. B. Unlu, "Analysis of laser parameters in the solution of photo-

acoustic wave equation," in Proc. SPIE **8581**, 858136-1 (2013, March), doi: 10.1117/12.2003844.

28. H. Erkol, E. Aytac-Kipergil, and M. B. Unlu, "Photoacoustic radiation force on a microbubble," Phys. Rev. E **90**, 023001 (2014), doi: 10.1103/PhysRevE.90.023001.

29. J. Xu, X. Wang, K. L. Cooper, and A. Wang, "Miniature all-silica fiber optic pressure and acoustic sensors," Opt. Lett. **30**, 3269-3271 (2005), doi: 10.1364/OL.30.003269.

30. J. Ma, *Miniature fiber-tip Fabry-Perot interferometric sensors for pressure and acoustic detection* (Doctoral dissertation, The Hong Kong Polytechnic University) (2014).

31. A. J. Oxenham and M. Wojtczak, "Frequency selectivity and masking. The Oxford," in *Handbook of Auditory Science: Hearing*, 5-44 (2010), doi: 10.1093/oxfordhb/9780199233557. 013.0002.

32. Q. Gong, Y. Wang, and M. Xian, "An objective assessment method for frequency selectivity of the human auditory system," Biomed. Eng. Online **13**, 171 (2014), doi: 10.1186/ 1475-925X-13-171.

33. Y. Ma, Y. He, X. Yu, C. Chen, R. Sun, and F. K. Tittel, "HCl ppb-level detection based on QEPAS sensor using a low resonance frequency quartz tuning fork," Sens. Actuators, B **233**, 388-393 (2016), doi:10.1016/j.snb.2016.04.114.

34. Z. Zhao, S. Nissila, O. Ahola, and R. Myllyla, "Production and detection theory of pulsed photoacoustic wave with maximum amplitude and minimum distortion in absorbing liquid," IEEE Trans. Instrum. Meas. **47**, 578-583 (1998), doi: 10.1109/19.744208.

35. L. V. Wang, "Ultrasound-mediumted biophotonic imaging: a review of acousto-optical tomography and photo-acoustic tomography," Dis. Markers **19**, 123-138 (2004), doi: 10.1155/ 2004/478079.

36. P. M. Morse and H. Feshbach, "Methods of theoretical physics," Am. J. Phys. **22**, 410-413 (1954), doi: 10.1119/ 1.1933765.

37. E. Aytac-Kipergil, H. Erkol, S. Kaya, G. Gulsen, and M. B. Unlu, "An analysis of beam parameters on proton-acoustic waves through an analytic approach," Phys. Med. Biol. **62**, 4694 (2017), doi: 10.1088/1361-6560/aa642c.

38. K. M. Quan, G. B. Christison, H. A. MacKenzie and P. Hodgson, "Glucose determination by a pulsed photoacoustic technique: an experimental study using a gelatin-based tissue phantom," Phys. Med. Biol. **38**, 1911 (1993), doi: 10.1088/ 0031-9155/38/12/014.